Properties of ^{26}Mg and ^{26}Si in the sd shell model and the determination of the ^{25}Al(p,γ)^{26}Si reaction rate

W. A. Richter, B. Alex Brown, A. Signoracci, and M. Wiescher

Phys. Rev. C **83**, 065803 — Published 10 June 2011

DOI: 10.1103/PhysRevC.83.065803

Properties of ^{26}Mg and ^{26}Si in the sd shell model and the determination of the ^{25}Al(p,γ)^{26}Si reaction rate*

W. A. Richter[1,2] B. Alex Brown[3], A. Signoracci[3] and M. Wiescher[4]
[1] *iThemba LABS, P.O.Box 722, Somerset West 7129, South Africa*
[2] *Department of Physics, University of the Western Cape, Private Bag X17, Bellville 7535, South Africa*
[3] *Department of Physics and Astronomy, and National Superconducting Cyclotron Laboratory, Michigan State University, East Lansing, Michigan 48824-1321, USA and*
[4] *Department of Physics and Joint Institute for Nuclear Astrophysics, University of Notre Dame, Notre Dame, IN 46556, USA*

We present theoretical results for the ^{25}Al(p,γ)^{26}Si resonance-capture rate. The isobaric mass multiplet equation is used to determined the energies and J^π values for of states in ^{26}Si based upon those observed in ^{26}Mg and ^{26}Al together with sd-shell calculations for the c-coefficients. Three Hamiltonians for the sd-shell, USD, USDA and USDB, are used to estimate the theoretical uncertainties in the gamma-decay and proton-decay widths that go into the resonance-capture rate.

PACS numbers: 26.30.-k, 21.60.Cs, 21.10.Sf, 21.10.Tg

I. INTRODUCTION

The production mechanism and production site for the long-lived radioactive isotope ^{26}Al has been of interest since the first indications of ^{26}Al enrichment in meteoritic inclusions was observed [1]. Understanding its origin would serve as a unique signature for nucleosynthesis in novae and supernovae. The main reaction sequence leading to ^{26}Al is ^{24}Mg(p,γ)^{25}Al($\beta^+ + \nu$)^{25}Mg(p,γ)^{26}Al. At the high-temperature conditions expected for shell carbon burning and explosive neon burning the ^{25}Al(p,γ)^{26}Si reaction becomes faster than the ^{25}Al β decay. Since ^{26}Si β decays to the short-lived 0^+ state of ^{26}Al, the production of the long-lived (5^+) state is by-passed.

In a recent paper [2] energies of levels in ^{26}Si were measured and used together with previous data and theoretical input to obtain a cross section for the ^{25}Al(p,γ)^{26}Si reaction. In previous work stellar rates were obtained using shell-model calculations and analog state information [3]. The current paper focuses on the theoretical aspects of the input and its uncertainties. The isobaric-mass-multiplet equation (IMME) is used to obtain the expected position of the levels in ^{26}Si based upon the observed energies of levels of the analogue states in ^{26}Al and ^{26}Mg, together with a calculation of the c-coefficient. The gamma and proton decay widths are calculated with several Hamiltonians to find their values and to estimate their theoretical uncertainties.

This paper follows from recent theoretical work on the properties of $(0d_{5/2}, 0d_{3/2}, 1s_{1/2})$ *sd*-shell nuclei that include new Hamiltonians [4], a comprehensive study of electromagnetic and beta-decay observables [5] and a comprehensive study of the properties of states in ^{26}Mg [6]. For ^{26}Mg assignments between theory and experiment for about 50 levels in ^{26}Mg levels up to 10 MeV in excitation have been made, based on a comparison of the experimental and theoretical level energies, electromagnetic transition strengths and electron scattering data [6].

In Sec. II we discuss the determination of the energies and J^π values for states in ^{26}Si based upon use of the IMME and related levels in ^{26}Mg and ^{26}Al. In Sec. III we show results for the resonance-capture rates based upon the USD, USDA and USDB Hamiltonians for the spectroscopic factors and gamma decay widths. In Sec. IV we discuss the results for various regions of temperature and the uncertainties for each region coming from the sd-shell Hamiltonians, the decay energies and the comparison with other related experimental data. Sec. V. we give a summary of our results and make comparisons to other recent results for this reaction rate.

II. PROCEDURE FOR DETERMINING ^{26}SI ENERGY LEVELS.

In the present work we make use of the IMME to calculate the expected energy of levels in ^{26}Si by using the measured binding energies of the $T = 1$ partners and a theoretical value of the c-coefficient of the IMME [7].

According to the IMME

$$B = a + bT_z + cT_z^2, \tag{1}$$

where B is the binding energy of a state. For the three $T = 1$ isobaric states in A=26 one can then write, with $T_z = (N - Z)/2$,

$$B_n = a + b + c, \tag{2}$$

where B_n applies to the neutron-rich member (^{26}Mg),

$$B_o = a, \tag{3}$$

for ^{26}Al and

$$B_p = a - b + c, \tag{4}$$

*This work was supported by NSF grant PHY-0758099 and Joint Institute for Nuclear Astrophysics, NSF-PFC

for the proton-rich member (^{26}Si). Then

$$c = (B_n + B_p - 2B_o)/2. \quad (5)$$

It also follows that

$$B_p = 2B_o - B_n + 2c. \quad (6)$$

For the calculation of the b- and c-coefficients of the IMME we use the USDB Hamiltonian [4] for the charge-independent part and add the Coulomb, charge-dependent and charge-asymmetric nuclear Hamiltonian obtained by Ormand and Brown for the *sd* shell [7]. For the nuclei considered in [7], A=18-22 and A=34-39, the 42 b-coefficients were reproduced with an rms deviation of 27 keV and the 26 c-coefficients were reproduced with an rms deviation of 9 keV. There is considerable state-dependence in the c-coefficients (ranging in values from 130 keV to 350 keV) that is nicely reproduced by the calculations (see Fig. 9 in [7]). In Fig. (1) values of c from experiment and theory are compared for $T = 1$ states $A = 26$ ordered according to increasing experimental energy. The experimental values are obtained for states where all three members of the multiplet are known. In general a good correspondence can be seen, the largest deviations being less than 30 keV. There is considerable state dependence with c values ranging from 300 keV (for the 0^+ ground state) down to 180 keV. This IMME method was used in [8] for the $T = 1$ states of the odd-odd nuclei with mass 28, 32 and 36. The agreement with experiment [Fig. (1)] for our even-even case appears to be better than obtained in [8] for the odd-odd cases.

Where data is not available in ^{26}Si to determine the c-coefficient from experiment, a value can be obtained from a theoretical calculation using Eq. (5). The binding energies for states in ^{26}Si can be then be obtained from Eq. (6), with experimental values of binding energy for corresponding states in ^{26}Al and ^{26}Mg (when they are known in both). Specifically

$$B_{\rm th}(^{26}{\rm Si}) = 2B_{\rm exp}(^{26}{\rm Al}) - B_{\rm exp}(^{26}{\rm Mg}) + 2c_{th}. \quad (7)$$

Figure (2) shows the typical assignment of states in ^{26}Si on the basis of known states in the mirror nucleus ^{26}Mg. Such assignments are indicated by dashed lines. The data are from Ref. [2]. There are shifts on the order of 300 keV. To improve on this procedure we determine ^{26}Si energies from Eq. (7). Fig. (3) shows the excitation energies for ^{26}Si obtained from Eq. (7) on the right compared to experiment on the left. The calculated values can then be used as a guide to the correct spin/parity assignments for measured levels in ^{26}Si. Where no levels in ^{26}Si are known, levels can be predicted. Two such levels (the 2^+ and 4^+) are indicated on the right-hand side of Fig. (3). The energy of the 3^+ state shown in the right-hand side of Fig. (3) was obtained from the average shift (250 keV) of the five highest states in Fig. (2). Above eight MeV where the property of states in ^{26}Mg ^{26}Al become uncertain we use the energies obtained from the USDB Hamiltonian. This includes the addition of about 170 states with $J^\pi \leq 5^+$ up to 14 MeV in excitation energy.

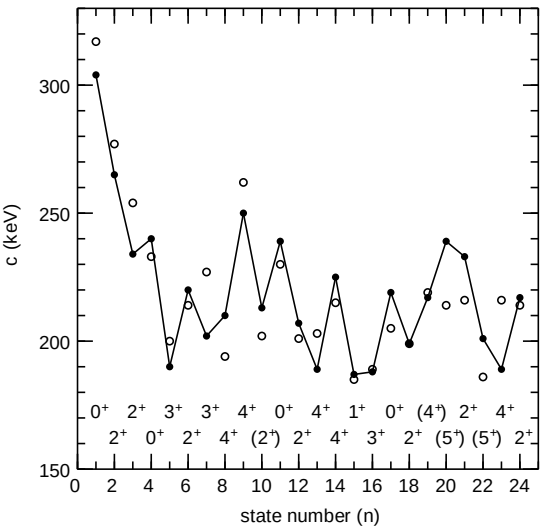

FIG. 1: c-coefficients from the isobaric mass multiplet equation (IMME: $E = a + bT_z + cT_z^2$) versus state number (in order of increasing energy) in ^{26}Si based on experimental energies (closed circles) and energies calculated from USDB (open circles).

The 0^+ state at 6.461 MeV [2] is much lower than the predicted energy of the fifth 0^+ state with USDB (at 8.040 MeV). It could be an intruder state. But, theory predicts the second 1^+ state (at 6.620 MeV) which has no experimental counterpart. For the purpose of the present calculations, we associate the theoretical second 1^+ state with the state observed at 6.461 MeV (see Table I). Our conclusions are insensitive to this choice.

The three levels that are just above the proton-decay separation energy of 5.51 MeV and of potential importance for the capture reaction at low temperatures are indicated by the arrows in Fig. (3). The J^π of levels 16 and 17 are from the recent analysis of Wrede [9] where arguments for the J^π are based on all available data for these states. This included the analysis of Bardayan et al. [10] for the ^{28}Si(p,t) data where an assignment $J^\pi = 2^+$ or 3^+ was made for state 16. From the associations made in Fig. (3) we can rule out 2^+.

III. RESULTS FOR THE REACTION RATE

The resonant reaction rate for capture on a nucleus in an initial state i, $N_A < \sigma v >_{{\rm res}\, i}$ for isolated narrow resonances is calculated as a sum over all relevant compound nucleus states f above the proton threshold [11]

$$N_A < \sigma v >_{{\rm res}\, i} = 1.540 \times 10^{11} (\mu T_9)^{-3/2}$$

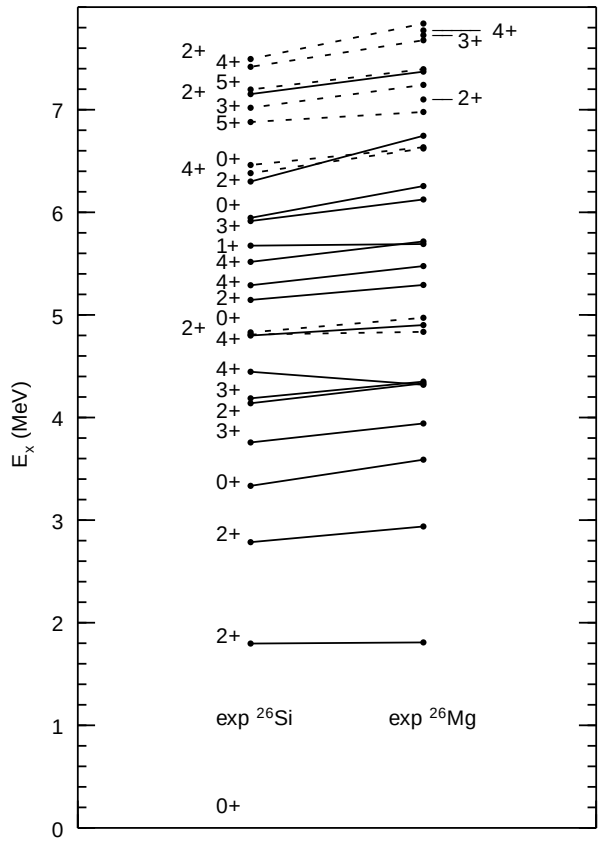

FIG. 2: Experimental excitation energies in ^{26}Si and ^{26}Mg [2]. Solid lines are for the states in ^{26}Si with firm J^π values. Dashed lines are for states in ^{26}Si with uncertain J^π values with the most likely mirror associations in ^{26}Mg with known J^π values. The three states indicated by lines to the right do not have known counterparts in ^{26}Si.

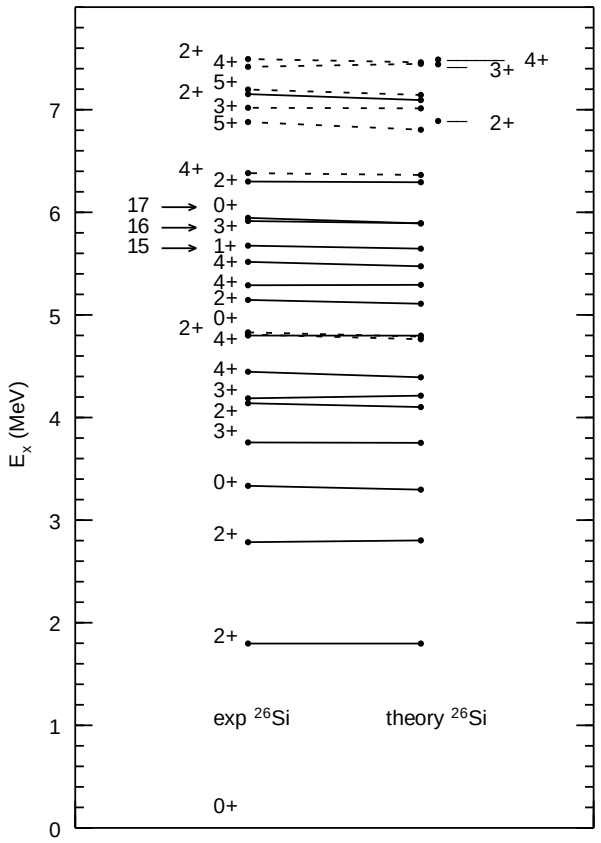

FIG. 3: Experimental excitation energies in ^{26}Si [2] versus predicted energies E_{th} based on Eq. (7). Dashed lines are for states in ^{26}Si with uncertain J^π values with the most likely mirror associations in ^{26}Mg with known J^π values. The three states indicated by lines to the right do not have known counterparts in ^{26}Mg. The energies of two of these (2^+ and 4^+) are based on the Eq. (7). The energy of the 3^+ is shifted down by 250 keV from its position in ^{26}Mg. Level number 20 in Table I is not shown in this figure (see the discussion in the text).

$$\times \sum_f \omega\gamma_{if}\ \ \mathrm{e}^{-\mathrm{E_{res}}/(kT)}\ \ \mathrm{cm^3\,s^{-1}mole^{-1}}. \qquad (8)$$

Here T_9 is the temperature in GigaK, $\mathrm{E}_{res} = \mathrm{E}_f - \mathrm{E}_i$ is the resonance energy in the center of mass system, the resonance strengths in MeV for proton capture are

$$\omega\gamma_{if} = \frac{(2J_f+1)}{(2J_p+1)(2J_i+1)}\frac{\Gamma_{\mathrm{p}\,if}\Gamma_{\gamma f}}{\Gamma_{\mathrm{total}\,f}}. \qquad (9)$$

$\Gamma_{\mathrm{total}\,f} = \Gamma_{\mathrm{p}\,if} + \Gamma_{\gamma f}$ is a total width of the resonance level and J_i, J_p and J_f are target (^{25}Al), the proton projectile ($J_p = 1/2$), and states in the final nucleus (^{26}Si), respectively. The proton decay width depends on the resonance energy via the single-particle proton width and can be calculated from the proton spectroscopic factor C^2S_{if} and the single-particle proton width $\Gamma_{\mathrm{sp}\,if}$ as $\Gamma_{\mathrm{p}\,if} = C^2S_{if}\Gamma_{\mathrm{sp}\,if}$. The single-particle proton widths were calculated from [12]

$$\Gamma_{\mathrm{sp}} = 2\gamma^2 P(\ell, R_c), \qquad (10)$$

with $\gamma^2 = \frac{\hbar^2c^2}{2\mu R_c^2}$ and where the ℓ-dependent channel radius R_c was chosen to match the widths obtained from an exact evaluation of the proton scattering cross section from a Woods-Saxon potential well for ^{25}Al for $Q = 0.1 - 0.4$ MeV. The simpler model of Eq. (10) matches the results obtained from the scattering cross sections as well as those used in [2] to within about 10%. We use a Coulomb penetration code from Barker [13].

The total resonance-capture reaction rates have been calculated for each of the interactions USD, USDA and USDB. We use the Q value of 5.5123(10) MeV from [14]. The energies for states in ^{26}Si are based on the results of Sec. II. The energies for the states up to eight MeV are given in the column labeled E_x(exp) in Table I.

Fig. (4) shows the results for the resonance-capture rate obtained using the properties of ^{26}Si given in Table I. The Γ_p and Γ_γ in this case are all based on the USDB

TABLE I: Properties of states up to eight MeV in ^{26}Si obtained with the USDB Hamiltonian. k is the number ordering for a given J^π value. The experimental energies are from Tables II and III of [2] except those as indicated by the footnotes.

n	J^π	k	E_x(USDB)	E_x(exp)	E_{res}	C^2S	C^2S	Γ_γ	Γ_p	$\omega\gamma$
			(MeV)	(MeV)	(MeV)	$\ell=0$	$\ell=2$	(eV)	(eV)	(eV)
1	0^+	1	0	0	0	0	2.5			
2	2^+	1	1.897	1.797		3.4×10^{-2}	3.6×10^{-1}	9.3×10^{-4}		
3	2^+	2	3.007	2.785		4.6×10^{-1}	8.0×10^{-2}	6.6×10^{-3}		
4	0^+	2	3.635	3.334		0	2.3×10^{-1}	1.2×10^{-4}		
5	3^+	1	3.883	3.757		2.7×10^{-1}	3.1×10^{-1}	3.7×10^{-4}		
6	2^+	3	4.450	4.139		2.4×10^{-2}	5.2×10^{-2}	1.1×10^{-2}		
7	3^+	2	4.317	4.187		7.0×10^{-2}	6.7×10^{-2}	7.7×10^{-3}		
8	4^+	1	4.365	4.446		0	8.5×10^{-2}	9.2×10^{-4}		
9	4^+	2	4.939	4.799		0	1.3×10^{-1}	1.3×10^{-2}		
10	2^+	4	4.883	4.809		6.3×10^{-2}	4.5×10^{-2}	1.0×10^{-2}		
11	0^+	3	5.033	4.830		0	4.0×10^{-2}	1.5×10^{-3}		
12	2^+	5	5.386	5.146		1.2×10^{-2}	4.6×10^{-1}	6.5×10^{-2}		
13	4^+	3	5.523	5.289		0	2.0×10^{-1}	2.0×10^{-2}		
14	4^+	4	5.893	5.517	0.005	0	3.6×10^{-2}	5.7×10^{-3}		
15	1^+	1	5.716	5.675	0.163	0	3.5×10^{-3}	1.2×10^{-1}	6.3×10^{-9}	1.6×10^{-9}
16	3^+	3	6.180	5.915	0.403	1.4×10^{-1}	3.3×10^{-1}	1.2×10^{-1}	3.5	6.8×10^{-2}
17	0^+	4	6.133	5.946	0.434	0	3.9×10^{-2}	8.8×10^{-3}	1.6×10^{-2}	4.7×10^{-4}
18	2^+	6	6.677	6.300	0.788	8.7×10^{-3}	1.0×10^{-1}	9.6×10^{-2}	5.3×10^{1}	4.0×10^{-2}
19	4^+	5	6.730	6.382	0.870	0	1.5×10^{-2}	2.4×10^{-2}	2.2	1.7×10^{-2}
20	1^+	2	6.620	6.461[a]	0.949	0	4.6×10^{-2}	1.1×10^{-1}	1.2×10^{1}	2.8×10^{-2}
21	5^+	1	7.068	6.880	1.368	0	1.4×10^{-2}	2.3×10^{-2}	4.0×10^{1}	2.1×10^{-2}
22	2^+	7	6.910	6.890[b]	1.378	5.7×10^{-4}	4.4×10^{-4}	1.2×10^{-1}	6.3×10^{1}	4.8×10^{-2}
23	3^+	4	7.296	7.019	1.507	3.9×10^{-3}	5.5×10^{-2}	2.1×10^{-1}	8.7×10^{2}	1.2×10^{-1}
24	2^+	8	7.149	7.152	1.640	4.5×10^{-2}	4.3×10^{-2}	7.3×10^{-2}	1.0×10^{4}	3.0×10^{-2}
25	5^+	2	7.388	7.197	1.685	0	1.0×10^{-2}	3.4×10^{-2}	9.0×10^{1}	3.1×10^{-2}
26	4^+	6	7.434	7.418	1.906	0	2.4×10^{-1}	2.2×10^{-1}	4.1×10^{3}	1.6×10^{-1}
27	3^+	5	7.699	7.442[c]	1.930	1.1×10^{-3}	4.7×10^{-2}	1.4×10^{-1}	1.3×10^{3}	8.4×10^{-2}
28	4^+	7	7.856	7.489[b]	1.977	0	5.7×10^{-2}	1.9×10^{-1}	1.1×10^{3}	1.4×10^{-1}
29	2^+	9	7.573	7.494	1.982	5.7×10^{-2}	1.0×10^{-1}	5.0×10^{-1}	2.8×10^{4}	2.1×10^{-1}

a) For this level which is assigned $J^\pi=0^+$ [2] we use the calculated values Γ_p and Γ_γ of the $J^\pi=1_2^+$ state.
b) The energies of these states observed in ^{26}Mg and not yet in ^{26}Si are taken from the present IMME calculations based on Eq. (7).
c) The energy of this state is based on its energy in ^{26}Mg with a downward shift of 250 keV that is the average of the upper five level shifts shown in Fig. (2).

Hamiltonian. In Fig. (5) we show some sensitivity studies. The upper two panels (a) and (b) show the results based on Γ_p and Γ_γ from the USDA and USD Hamiltonians relative to USDB. In panel (c) we compare the rate obtained when the theoretical $\Gamma_\gamma(^{26}\mathrm{Si})$ are replaced by $\Gamma_\gamma(^{26}\mathrm{Mg})$ with the excitation energies the same in both cases. These Γ_γ differ because the electromagnetic matrix elements have a small mirror asymmetry. This comparison shows that at the level of 10% it is adequate to take the Γ_γ information from the mirror nucleus when it is known. One could also correct for gamma-decay phase-space change due to the difference in excitation energies between the mirror nuclei [Fig. (2)]. This correction is typically less than 10% and will not be included here.

IV. UNCERTAINTIES IN THE RESONANT CAPTURE REACTION RATES

In this section we discuss the uncertainties for the various regions of temperature and the resulting recommendations for the rate and error. In addition to the uncertainties coming from Γ_γ and the spectroscopic factors, there are uncertainties related to the reaction Q values for Γ_p and the E_{res} dependence in Eq. (8). We use Q_0^{new} = 5.5123 MeV from [14]. As discussed in [14] it differs

by 5 keV from the older results $Q_0^{old} = 5.5177$ MeV. The excitation energy error for the two levels just above the proton-decay threshold are [2] 2.2 keV for the 5.675 MeV 1^+ state and 1.8 keV for the 5.916 MeV 3^+ state. In order to estimate the energy uncertainty in the capture rate we redo the rate calculation with a 5 keV higher Q value. The results for the ratio are shown in Fig. (6).

A. Region of Log(T9) < -0.8

For these lowest T9 values the resonance-capture rate comes entirely from the 5.675 MeV 1^+ state (number 15 in Table I). Since $\Gamma_\gamma >> \Gamma_p$ for this case the rate is determined by Γ_p. The large change shown on the left-hand side of panels (a) and (b) in Fig. (5) is due to the change in the relatively small spectroscopic factors; 0.0048 (USDB), 0.0027 (USDA) and 0.0035 (USD). For this region of T9 we recommend the USD rate with an uncertainty of 40% coming from the spread of the theoretical spectroscopic factors. From Fig. (6) the uncertainty in the rate from the Q value uncertainties are on the order of 50%.

The direct-capture rate become important below log(T9) of about -1.5 [below the scale of Fig. (4).] For comparison to other results discussed in the next section we use the direct-capture rate taken from Table VII of [2]. This is based on the USDB spectroscopic factors for the bound states in Table I. The uncertainty in the direct-capture rate is about 20% since the USD Hamiltonians give spectroscopic factors for these bound states that are the same within about 20%.

B. Region of $-0.7 <$ Log(T9) < 0.5

The resonance capture rate in this region is dominated by the properties of the 3^+ state at 5.915 MeV (number 16 in Table I). Since $\Gamma_\gamma < \Gamma_p$ the rate is determined by Γ_γ.

The gamma-decay half-life of the analogue 3^+ level in the mirror nucleus ^{26}Mg has been measured [15]. Experiment and theory are compared in Table II which also includes some results for other states above 5.8 MeV. Experiment and theory are compared for lower energy states of ^{26}Mg in Table I and Fig. (2) of [6].

The experimental half-life of this 3^+ level in ^{26}Mg of 14(6) ps [15] is larger than the USDB result of 4.0 ps. The USDA and USD values for the half-life are 4.5 and 5.0 fs, respectively. Based on the comparisons shown in Fig. (2) of [6] for the lifetimes of other levels in ^{26}Mg above five MeV (levels 10-22), this deviation is larger than expected. However, the experimental uncertainty is relatively large for this lifetime. It has only been measured once by the doppler shirt attenuation method [15]. Thus, we choose to use the USDB value. It would be important to improve the experimental uncertainty in this lifetime. In addition, one could measure the gamma-decay decay branching for the 403 keV resonance in ^{26}Si which is predicted to be 3% relative to proton decay.

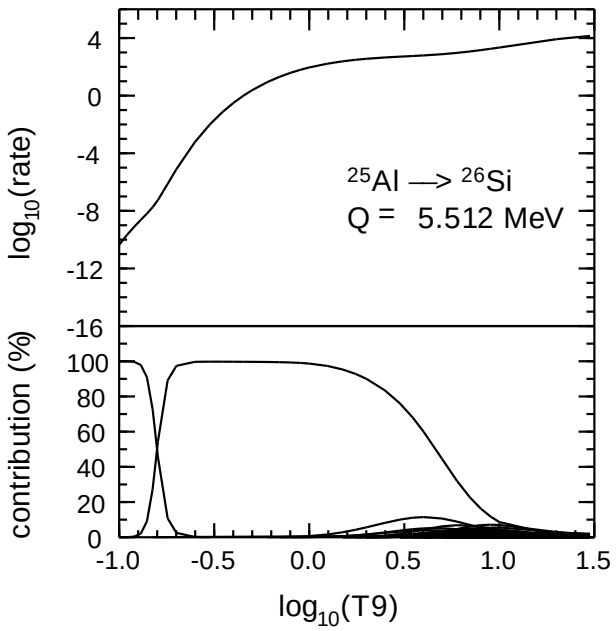

FIG. 4: The total resonance-capture reaction rate versus temperature T9 (GigaK) (top panel) and the contribution of each of the final states (lower panel) with USDB. In the lower panel the dominant contribution below log(T9) $= -0.8$ is from state number 15, the 1^+ state at 5.675 MeV. Between log(T9) $= -0.7$ and 0.5 the dominant contribution is from state number 16, the 3^+ state at 5.915 MeV.

The theoretical uncertainty for this energy range coming from Γ_γ is about 20%. But as discussed above, one should confirm the experimental result for ^{26}Mg which deviates from the theory outside of this error. In the lower end of this temperature range there is an uncertainty of about 40% coming from a possible Q value error of 5 keV.

C. Region of 0.7 $<$ Log(T9)

For log(T9) > 0.7 the rate comes from the contribution of many states with $\Gamma_\gamma << \Gamma_p$. The $\omega\gamma$ depends on the $(2J_f + 1)$ level density and the associated Γ_γ. In Fig. (7) we show the result for log(T9)=1. $\omega\gamma$ increases exponentially due to increasing level density, but with the exponential factor $\exp(-E_{res}/kT)$ about 80% of the total contribution comes from states below 10 MeV in excitation energy ($E_{res} = 4.5$ MeV). The sd-shell provides a fairly realistic model for the positive-parity level density up to 10 MeV, but there will be contributions from pf shell intruder states starting with the possible state at 7.2 MeV in ^{26}Mg [6]. Starting with the known 3^- state in ^{26}Mg at 6.8 MeV there will be contributions

TABLE II: Properties of some states in ^{26}Mg.

J^π	k	E_x(USDB)	E_x(exp)	$T_{1/2}$(USDB)	$T_{1/2}$(exp) [16]	Γ_γ(USDB)	Γ_γ(exp)
		(MeV)	(MeV)	(fs)	(fs)	(eV)	(ev)
1^+	1	5.716	5.691	3.1	<8	0.147	<0.06
3^+	3	6.180	6.124	4.0	14(6)	0.114	$0.033^{+0.024}_{-0.10}$
0^+	4	6.133	6.256	58	52(24)	0.0078	$0.009^{+0.007}_{-0.003}$
2^+	6	6.677	6.745	5.3	16(8)	0.086	$0.028^{+0.028}_{-0.009}$
4^+	5	6.730	6.622	20	19(5)	0.023	$0.024^{+0.009}_{-0.005}$
$(0-4)^+$	2	$6.620(1^+)^a$	6.634	4.4	<7	0.104	<0.06
2^+	7	6.910	6.746	3.2	16(8)	0.143	$0.028^{+0.028}_{-0.009}$

a) For this level which is assigned J^π=$(0-4)^+$ [16] we use the calculated value for the J^π=1^+ state at 6.620 MeV.

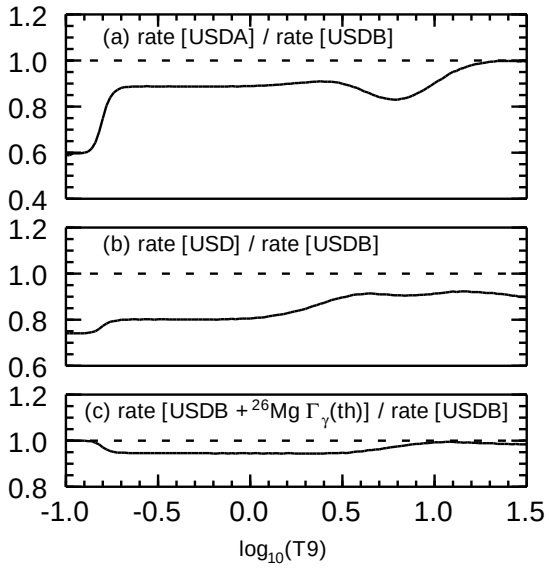

FIG. 5: Rates calculated with different assumptions divided by the USDB results given in Fig. (4).

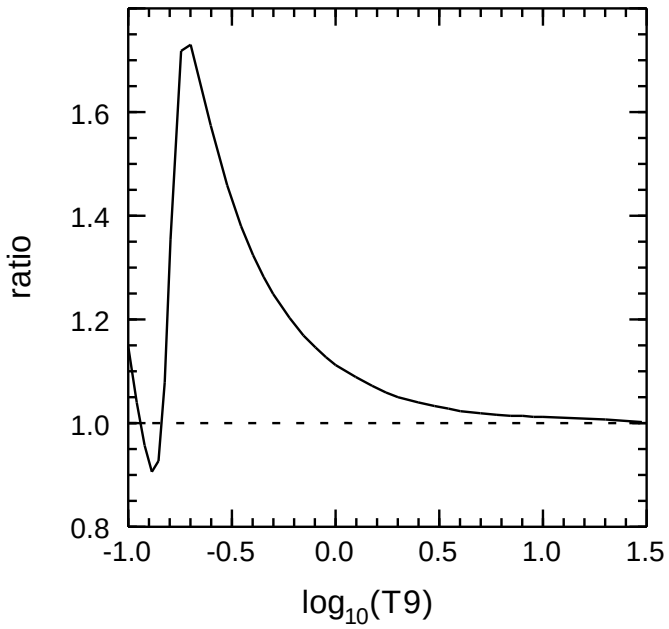

FIG. 6: The ratio given by the rate calculated with Q = 5.5123 MeV divided by the rate obtained with Q = 5.5173 MeV.

from negative-parity states. At log(T9)=1 we estimate that the effective level density and the effective rate is about a factor of two higher than that given by the sd-shell model. Above log(T9) = 1 one should base the rate on a Hauser-Feshbach formulation with level densities adjusted to match the known level density in the region of 6−9 MeV excitation energy.

V. DISCUSSION AND CONCLUSION

The calculation the reaction rate for ^{25}Al(p,γ)^{26}Si requires a knowledge of the levels in ^{26}Si. The experimental properties of levels in ^{26}Si are uncertain and incomplete compared to those in the mirror nucleus ^{26}Mg. In cases where the analogue $T = 1$ levels are known in both ^{26}Mg and ^{26}Al we use the IMME with the c-coefficient calculated from theory in order to predict the level properties of ^{26}Si. For levels where all three member of the isobaric triplet are known we find good agreement between the calculated and theoretical c coefficients. For the higher states we can affirm some of the spin assignments for known levels in ^{26}Si, and predict the location of several levels not yet observed up to 7.6 MeV. We obtained the spectroscopic factors and gamma decay lifetimes for rate calculations from shell-model calculations using the USD sd-shell Hamiltonian as well as the newer USDA and USDB Hamiltonians. Reaction rates as well as contributions from individual states in ^{26}Si were then obtained for the different interactions. The variation in the rates calculated give an indication of the theoretical

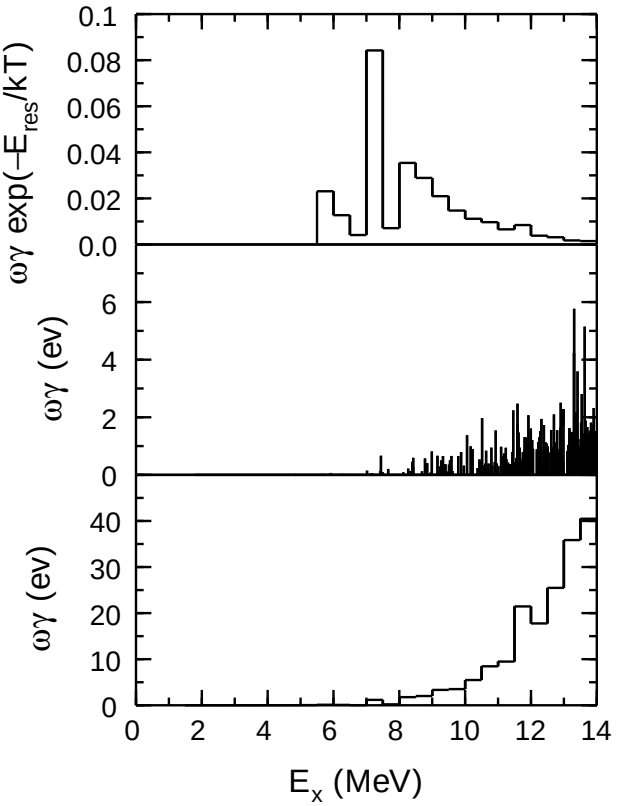

FIG. 7: Relative contributions to the rate for log(T9) = 10. The top and bottom curves are binned over 0.5 MeV to show the integrated contribution for each bin. The middle curve shows the contribution from individual states.

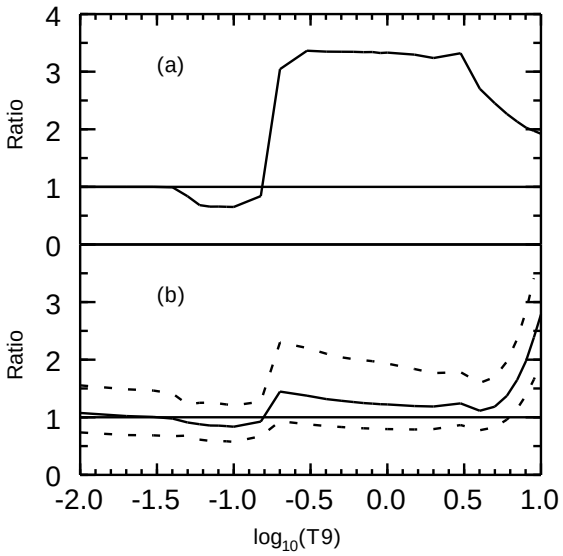

FIG. 8: (a) The present rate divided by the rate given in Table VII of [2]. (b) The present rate divided by the rate given in the 2010 evaluation (Table B.37 of [17]); solid line for the Median rate and the dashed lines for the low and high rates.

uncertainty. It was shown that using theoretical gamma widths from the mirror nucleus ^{26}Mg instead of ^{26}Si is an adequate approximation.

We have discussed the problem that the experimental gamma-decay lifetime of the 6.124 MeV 3^+ level in ^{26}Mg of 14(6) fs is larger than the theoretical USDB value of 4.0 fs. For the resonant-capture rate we use the gamma-decay width in ^{26}Si from the USDB calculation. The lifetime in ^{26}Mg has only been measured once [15]. It would be important to improve the experimental uncertainty in this lifetime. In addition, one should try to measure the gamma-decay decay branching for the 403 keV resonance in ^{26}Si which is predicted to be 3% relative to proton decay.

Our final ^{25}Al(p,γ)^{26}Si rate is compared to that of Matic et al. [2] and to the rate recommended in the 2010 Evaluation of Monte Carlo based Thermonuclear Reaction Rates [17] in Fig. (8). In the region of log(T9) = -0.7 to 0.7 our rate is a factor of about three higher than Matic et al. due to the fact that they use the experimental value of the 3^+ lifetime in ^{26}Mg. We have discussed in Sec. IV.B the reason for our preference for using the theoretical value.

Above log(T9) of 0.5 our cross section increases relative to [2] and [17] since we include more positive-parity sd-shell levels. But above log(T9) of about 0.8 our cross section is still a lower limit since negative-parity states have not been included.

Below log(T9) of 0.8 our results are consistent with the Monte Carlo based Thermonuclear Reaction Rates [17]. We note that these rates use the spectroscopic factors and Γ_γ obtained from the USD Hamiltonian. As we have shown, the values obtained with USDB are within 20% of those obtained with USD, with the exception of the spectroscopic factor for the 1^+ state just above threshold for which we use the USD value with a 40% error accounting for the spread between USD, USDA and USDB.

The astrophysical implications for novae and x-ray bursts in terms of the competition between the ^{25}Al(p,γ)^{26}Si and the ^{25}Al β decay rates is shown in Fig. (9) of [2]. Our factor of three higher rate for ^{25}Al(p,γ)^{26}Si compared to that of [2] in the temperature range of interest, log(T9)=0.1-0.3, will relatively reduce the population of the long-lived 5^+ state of ^{26}Al by bypassing its production. It would be interesting to apply these new rates to various astrophysical scenarios to find the quantitative consequences.

For the next generation of rp capture cross section calculations it will be important to consider theoretical errors coming from uncertainties within the model-space assumptions as well as those that come from the limitations of the model-space truncations.

Acknowledgments This work is partly supported by NSF Grant PHY-0758099, NSF Grant No. PHY08-22648 (Joint Institute for Nuclear Astrophysics), and the Na-

tional Research Foundation of South Africa.

[1] T. Lee, D. A. Papanantassiou and G. J. Wasserburg, Astrophys. J. Lett. **211**, L107 (1977); **220**, L21 (1978).
[2] A. Matic et al., Phys. Rev. C **82**, 025807 (2010).
[3] C. Iliadis, L. Buchman, P. M. Endt, H. Herndl and M. Wiescher, Phys. Rev. C **53**, 475 (1996)
[4] B. A. Brown and W. A. Richter, Phys. Rev. C **74**, 034315 (2006).
[5] W. A. Richter, S. Mkhize and B. A. Brown, Phys. Rev. C **78**, 064302-1 (2008).
[6] W. A. Richter and B. A. Brown, Phys. Rev. C **80**, 034301 (2009).
[7] W. E. Ormand and B. A. Brown, Nucl. Phys. A **491**, 1 (1989).
[8] C. Iliadis, P. M. Endt, N. Prantzos and W. J. Thompson, The Astrophysical Jour. **524**, 434 (1999).
[9] C. Wrede, Phys. Rev. C **79**, 035803 (2009).
[10] D. W. Bardayan et al., Phys. Rev. C **74**, 045804 (2006).
[11] W. A. Fowler and F. Hoyle, Ap. J. Suppl. **9**, 201 (1964).
[12] A. M. Lane and R. G. Thomas, Rev. Mod. Phys. **30**, 257 (1958).
[13] F. C. Barker, Phys. Rev. C **63**, 047303 (2001); and private communication.
[14] A. Parikh, J. A. Caggiano, C. Deibel, J. P. Greene, R. Lewis, P. D. Parker and C. Wrede, Phys. Rev. C **71**, 055804 (2005).
[15] F. Glatz, S. Norbert, E. Bitterwolf, A. Burkard, F. Heidinger, Th. Kern, R. Lehmann, H. Ropke, J. Siefert and C. Schneider, Z. Phys. A **324**, 187 (1986).
[16] http://www.nndc.bnl.gov/ (2010).
[17] C. Iliadis, R. Longland, A. E. Champagne, A. Coc and R. Fitzgerald, Nucl. Phys. **A841**, 31 (2010).